



# Sensitivity of atom based on slow light propagation and rotary photon drag: an efficient and secure model for quantum-based sensors in Internet of Things

Syed Sajid Ullah<sup>1</sup> · Aizaz Khan<sup>2</sup> · Saddam Hussain<sup>3</sup> · Majed Alsafyani<sup>4</sup> · Roobaea Alroobaea<sup>4</sup> · Sultan Algarni<sup>5</sup>

Received: 15 July 2023 / Accepted: 4 October 2023 / Published online: 8 November 2023  
© The Author(s) 2023

## Abstract

Quantum technology has the potential to revolutionize sensors and the Internet of Things (IoT). Efficient and secure data transfer among sensors and IoT devices is a major challenge. To address this, the manuscript presents coherent manipulation of the scattering cross section and its sensitivity based on subluminal propagation and rotary photon drag, using an atomic medium with two levels coupled with a cavity. The group index of the proposed atomic medium is measured in the range of  $-0.1 \leq n_g \leq 150$  and group velocity in the range of  $2 \times 10^6 \text{ m/s} \leq v_g \leq \pm 2 \times 10^9 \text{ m/s}$ . The maximum delay time is reported to  $t_g = 0.3 \mu\text{s}$  and rotary photon drag to  $\theta_d = \pm 5$  micro radian. This effect of photon drag is used in sensing, energy harvesting, and optical switching in IoT. The scattering cross-section of  $0.1 \times 10^{21} \text{ m}^2$  is reported. The scattering cross-section impacts the efficiency and reliability of quantum-based communication for IoT. The maximum cross-sectional sensitivity is measured to  $S_\sigma = 0.4 \times 10^{-19} \text{ m}^2/n_r$ . The cross-sectional sensitivity potentially impacts secure communication and highly precise detection in sensors and IoT.

**keywords** Quantum Technology · Quantum-based Sensors · Quantum for Internet of Things · Quantum Effects

## 1 Introduction

Recently, Quantum technology has the potential to revolutionize sensors and the Internet of Things (IoT). Different quantum techniques are used to integrate quantum sensors, quantum devices, algorithms, and protocols into IoT systems to enhance their capabilities and address certain communications challenges (Chawla and Mehra 2023). The light (electromagnetic waves) is used as a medium in these quantum techniques for signal processing and data transfer among sensors, IoT devices, and end users (Karim et al. 2023). Still, it raises many challenges, such as efficient single processing, security, precision, energy harvesting, streaming, sensing, and real-time communications. The rapid invention of these quantum-based IoT devices and communication, requires an advanced quantum model that effectively addresses the mentioned challenges (Ageed et al. 2022). Many effects such as

photon drag, scattering cross-section, and cross-sectional sensitivity of atoms under the quantum-based model, are used to solve these challenges.

Photon drag is a phenomenon where a lateral displacement (drag) is experienced in the direction of propagating light beam through a moving medium. In photon drag, a force is exerted on a particle when it is subjected to a light gradient or a laser beam (Saushin et al. 2021). For quantum-based IoT, photon drag is practical in IoT applications, sensing and detection, energy harvesting, and optical switching. In IoT devices, photon drag can be utilized by exploiting the force exerted on particles due to the light gradient; it detects and senses many parameters (Butt et al. 2023). This property can be harnessed to create susceptible and compact sensors for various IoT applications, including environmental monitoring, healthcare, or industrial automation. Photon drag has potential applications in energy harvesting purposes for IoT devices. A particle experiences an induced force due to an external field (light) gradient, creating mechanical motion. The mechanical motion is then converted into electrical energy, generating energy from an ambient light source. The generated energy is used in low-power IoT devices and sensors. In optical switching, an external field (mostly a laser beam) exerts a force on the atoms which is used for the manipulation of the position as well as the movement of these atoms. Based on this property, optical switches (re-configurable optics) are made for IoT devices and used for the control and modulation of signals dynamically.

The scattering cross-section is a concept commonly used in quantum to describe the interaction of electromagnetic waves with particles or objects. In quantum-based IoT, there are instances where electromagnetic waves interact with objects or structures, resulting in various phenomena such as signal attenuation, reflection, or interference. These interactions impact the efficiency and reliability of wireless communication systems and quantum-based IoT devices (Chawla and Mehra 2023; Costa et al. 2020).

The cross-sectional sensitivity of atoms in the context of quantum-based IoT refers to the ability of atoms or other quantum systems to detect and respond to external influences with high precision. In quantum-based IoT (Li et al. 2023), atoms are often utilized as the building blocks for quantum sensors that can measure physical quantities such as magnetic fields, electric fields, temperature, and pressure at the quantum level, by carefully controlling and manipulating the quantum states of atoms. Furthermore, quantum systems like atoms can also enable secure communication in quantum-based IoT. Quantum cryptography techniques, such as quantum key distribution (QKD) (Xu et al. 2023) utilize the quantum properties of atoms or other quantum systems to establish secure communication channels highly resistant to eavesdropping.

Motivated from the forth-mentioned discussion, sensitivity of atom based on slow light propagation and rotary photon drag: an efficient and secure model for quantum-based sensors in IoT. The major contributions of the proposed research work are as follows;

- We used an atomic medium, having two levels coupled with a cavity, to manipulate the scattering cross-section and its sensitivity.
- We provided a detailed network and quantum atomic model.
- In our proposed model, the value of the group index is measured in the range of  $-0.1$  to  $150$
- We modified the group velocity, having a value of  $2 \times 10^6$  m/s to  $\pm 2 \times 10^9$  m/s, which enhances the speed of information transfer in IoT under a quantum-based communication.
- We found that the proposed medium had a delay time of  $t_d = 0.3$   $\mu$ s, which increased the storage capacity of information related to the IoT.

- The rotary photon drag of  $\theta_d = \pm 5$  micro radian is obtained and used in highly sensitive and compact sensing, energy harvesting, and proper optical switching in IoT.
- We reported the scattering cross-section of  $0.1 \times 10^{21} m^2$  having an impact on the efficiency and reliability of quantum-based communication for IoT.
- We were able to attain a maximum cross-sectional sensitivity of  $S_\sigma = 0.4 \times 10^{-19} m^2/n_r$ , which has the potential to have an impact on secure communication as well as high precision detection in sensors and the IoT.
- We provided deployment and workflow for the proposed model in sensors and IoT.

## 2 Network and atomic models

This section discusses the following sensors and IoT-based network models and the Quantum atomic model.

### 2.1 Network model

In Fig. 1, the proposed sensors and network model are shown. The proposed model has entities: Quantum-based sensors, sender-side quantum-based IoT devices, Receiver-side quantum-based IoT devices, quantum security providers, quantum keys and state detectors, and quantum towers. The detail and work process of every entity is explained as follow:

- *Quantum-based Sensors* These are tiny devices that sense and detect environmental changes, healthcare, infrastructure management, industries, and many more IoT ecosystems by using quantum techniques.
- *Sender Side Quantum Based IoT Devices* These devices transmit information collected from sensors using our proposed quantum-based model. The proposed model and techniques ensure secure and efficient data transfer in IoT devices.

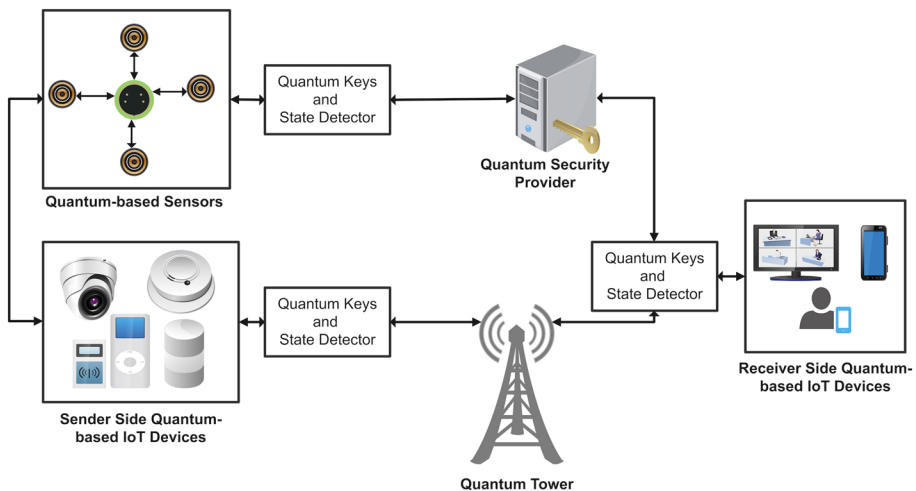


Fig. 1 Sensors and IoT-based network model

- *Receiver Side Quantum Based IoT Devices* These devices receive the information transferred by Sender Side Quantum Based IoT Devices.
- *Quantum Security Provider* A trustable third party that is responsible for secure communication among participating entities in the IoT network. For security, it generates quantum keys and states using quantum cryptography.
- *Quantum Keys and State Detector* This detector is used to verify quantum keys and states for sensors and IoT devices.
- *Quantum Tower* For long-distance communication, it transfers information and signals among entities based on quantum techniques.

All the above-mentioned entities are to be used case of our designed scheme. At first, the quantum-based sensors use our photon drag investigation by exploiting the force exerted on particles due to the light gradient to efficiently sense and monitor the environment. This sensing data then transfers to the receiver-side quantum-based IoT devices, this transfer will be possible through a quantum tower and optical switching. To make this transfer efficient, the proposed photon drag technique is a very efficient solution to boost the performance of optical switching. Our photon drag exerts a force on the atoms that are used to manipulate the position and move the atoms, which provides higher bandwidth compared to traditional ones, enables the transfer of bulk data, makes possible HD-streaming, and can handle data from multiple sources, at the same time.

For long-distance communications, an intermediate quantum tower is used to transfer data. Our technique the scattering cross-section is an efficient solution for efficient and reliable long-distance communications. The scattering cross-section refers to the phenomenon describing the interaction between electromagnetic waves and particles/atoms, that reduces the blockage of signals, increases its propagation, handles multi-path fading, and reduces to avoid conjunction. Strong security is a highlighted issue in any quantum-based communication, a quantum security provider is used to manage the security. The quantum security provider provides keys for secure communication. These keys will be a combination of the photons, to verify and validate keys through quantum states, quantum keys and state detectors are used. Our proposed cross-sectional sensitivity investigation is utilized to increase security. The cross-sectional sensitivity of atoms in the context of quantum-based IoT refers to the ability of atoms to detect and respond to external influences with high precision that boosts up security and makes efficient quantum key distribution and detection process.

## 2.2 Atomic model

As illustrated in Fig. 2, our suggested model consists of a two-level atomic medium coupled with a single-mode cavity. Dielectric slabs of a thickness  $d_1$  and an inter-slab space of  $d_2$  make up the walls. The ground state of the two-level atoms is labelled as  $|1\rangle$  while the excited state as  $|2\rangle$ . A probe field having Rabi frequency  $\Omega_p$ , that makes an angle  $\theta$  with the normal is shined from one side of the cavity. Strong control field having Rabi frequency  $\Omega_c$  is driven normally from a single side of the cavity. Considering the ground state at zero energy level, the Hamiltonian under dipole and rotatory wave approximation is then given by Arif et al. (2021)

$$H = \hbar\omega_{21}|2\rangle\langle 2| + \hbar va^\dagger a + \hbar G(a^\dagger \sigma_{12} + a\sigma_{21}) - \frac{\hbar}{2}(\Omega_c e^{-i\omega_c t} \sigma_{21} + \Omega_p e^{-i\omega_p t} \sigma_{21} + H.C) \quad (1)$$

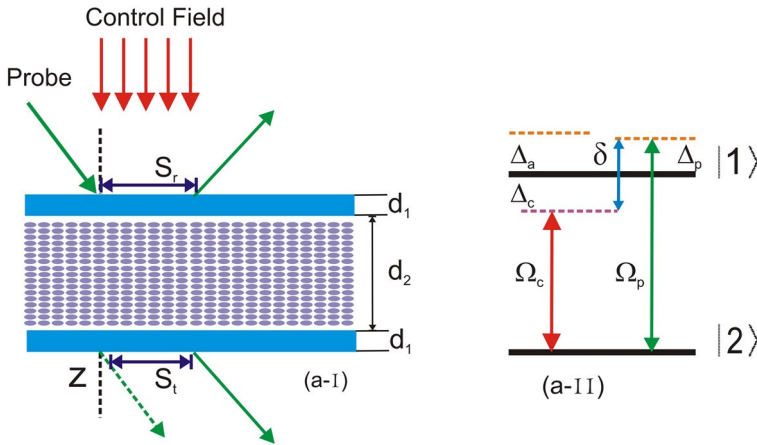


**Fig. 2** a-I The cavity containing a two-level atomic medium where the red arrows indicate the control field while green arrows show the probe field. a-II The energy level diagram with control and probe fields as well as detuning

The control field is detuned from the probe field, and atomic transition frequency  $\omega_{21}$  by an amount  $\delta = \omega_{21} - \omega_c$  and  $\Delta_a = \omega_p - \omega_c$ , respectively. Similarly, the detuning of cavity mode  $\nu$  and probe field from atomic transition frequency is given by  $\Delta_c = -(\omega_{21} - \nu)$  and  $\Delta_p = \omega_{21} - \omega_p$ , respectively. Whereas,  $\omega_c$  and  $\omega_p$  are the angular frequencies of the control and probe fields, respectively. In the above equation,  $G$  is the coupling strength between the system and cavity mode,  $a^\dagger(a)$  are the creation and annihilation operators for the cavity mode. The  $a$  is the lowering operator for the atomic decays between states of the proposed atomic model while  $a^\dagger$  is the raising operator for these decays. Furthermore,  $\sigma_{ij}$  is the operator for atomic transition while  $\Omega_{c,p}$  are the Rabi frequencies of the driving fields. The parameter  $\rho$  having the dimensions of frequency is the strength of the atom cavity coupling, given in explicit form as  $\rho = \mu_{21}\zeta_V/\hbar$ , where  $\mu_{21}$  is the transition dipole moment and  $\zeta_V = [(\hbar\nu)/2\hbar\epsilon_0 V]^{1/2}$  is the strength of vacuum field over the volume  $V\epsilon$  of the cavity. To study the dynamics and equation of motion for the proposed system, we use the following master equation (Arif et al. 2021).

$$\dot{\rho} = -\frac{i}{\hbar}[H, \rho] - \frac{1}{2}\gamma(\alpha^\dagger\alpha\rho + \rho\alpha^\dagger\alpha - 2\alpha\rho\alpha^\dagger) \tag{2}$$

Where  $\hbar$  is reduced plank constant,  $\rho$  is the density matrix operator and  $\gamma$  is the damping rate. Using Eqs. (1) and (2), we obtained the following equations which describe the dynamics of the population, as well as polarization.

$$\dot{\rho}_{22} = iG\sqrt{1+n} + \frac{1}{2}(\Omega_c + \Omega_p e^{-i\delta t})\rho_{12} - iG\sqrt{1+n} + \frac{1}{2}(\Omega_c^* + \Omega_p^* e^{-i\Delta t})\rho_{21} - \gamma\rho_{22} \tag{3}$$

$$\dot{\rho}_{12} = i(\Delta_a + \Delta_c - \gamma/2)\rho_{12} - iG\sqrt{1+n} + \frac{1}{2}(\Omega_c^* + \Omega_p^* e^{-i\Delta t})(\rho_{11} - \rho_{12}) \tag{4}$$

Where,  $\dot{\rho}_{21} = \dot{\rho}_{12}^*$ ,  $\dot{\rho}_{11} = -\dot{\rho}_{22}$  and  $n$  is the number of photons in the cavity mode. The exact steady-state solutions of the above equations are obtained by applying the following possible solutions to each of them.

$$\rho_{uv} = \rho_{uv}^0 + \rho_{uv}^+ e^{i\delta t} + \rho_{uv}^- e^{-i\delta t} \tag{5}$$

We have used the rotating wave approximation, assuming that the detuning between the atomic transition frequency  $\delta$  and the cavity frequency is much larger than the decay rate  $\gamma$  of the atomic states. In the above equation,  $\rho_{uv}^0$  is the steady state solution under atom coupling with  $\Omega_c$  and  $\delta$ . The preceding two terms describe the steady-state solution in the presence of coupled probe field. Utilizing this equation and comparing constants and coefficients of the exponential yields twelve coupled equations; the first order coherence  $\rho_{21}^-$  in  $\Omega_p$  is given by:

$$\rho_{21}^- = \frac{(\gamma + 2i(\Delta_a + \Delta_c))\Omega_p(A_1 + A_2 - 2\delta(2\rho\sqrt{1+n} + \Omega_c)\Omega_c^*)}{(A_3 + (2\rho\sqrt{1+n} + \Omega_c)\Omega_c^*)(A_4 + 4\rho\sqrt{1+n}(\gamma - 2i\delta)\Omega_c + 2(\gamma - 2i\delta)(2\rho\sqrt{1+n} + \Omega_c)\Omega_c^*)} \tag{6}$$

The terms in the above equations are given below.

$$\begin{aligned} A_1 &= i\gamma^3 + \gamma^2[3\delta + 4(\Delta_c + \Delta_a)] - 2i\gamma[\delta^2 + 4\delta(\Delta_c + \Delta_a) + 2(\Delta_c + \Delta_a)^2] \\ A_2 &= -4\delta[(1+n)2G^2 + (\delta + \Delta_a + \Delta_c)(\Delta_c + \Delta_a) + G\sqrt{1+n}\Omega_c^2] \\ A_3 &= 4G^2[1+n] + \gamma^2 + 4\Delta_a^2 + 8\Delta_c\Delta_a + 4\Delta_c^2 + 2G\sqrt{1+n}\Omega_c \\ A_4 &= 8G^2[(\gamma - 2i\delta)(1+n)] + (\gamma - i\delta)[\gamma^2 - 4i\gamma\delta + 4(-\delta^2 + (\Delta_a + \Delta_c)^2)] \end{aligned}$$

Where

$$\begin{aligned} T_1 &= (A_1 + A_2 - 2\Delta(2G\sqrt{1+n} + \Omega_c)\Omega_c^*) \\ T_2 &= (A_3 + (2G\sqrt{1+n} + \Omega_c)\Omega_c^*) \\ T_3 &= (\gamma - 2i\Delta)(2G\sqrt{1+n} + \Omega_c)\Omega_c^* \end{aligned}$$

To access the susceptibility in terms of position-dependent Rabi frequency of the control driving field  $\Omega_c(kx, ky)$ , we define the induced polarization in terms of susceptibility and electric probe field of amplitude  $E_p$  as  $p = \epsilon_0\chi_e E_p$  and in terms of the probe field coherence  $\rho_{21}$ , it is given by  $p = 2N\mu_{21}\rho_{21}$ , where  $N$  is the atomic density. Comparing these relations, while assuming  $\rho_{21}^- = \rho_{21}$  the susceptibility of the intra-cavity medium becomes:

$$\chi = \beta \frac{(\gamma + 2i(\Delta_a + \Delta_c))T_1}{T_2(A_4 + 4G\sqrt{1+n}(\gamma - 2i\Delta)\Omega_c + 2T_3)} \tag{7}$$

where  $\beta = \frac{2N|\mu_{21}|^2}{\epsilon_0\hbar}$ . The refractive index is calculated by  $n_r = 1 + 2\pi Re(\chi)$ .

The group index is written as:

$$n_g = n_r + \omega \frac{\partial(n_r)}{\partial\omega} \tag{8}$$

The velocity at which, information is transferred along a wave is the group velocity. The group velocity in terms of group index is written as:

$$v_g = \frac{c}{n_g} \quad (9)$$

The delay time is the difference of time taken by a light beam in a medium to the time taken in vacuum for the same length  $L$ , i.e.  $t_d = t_m - t_v$ . In context of group index, it can be written as:

$$t_g = \frac{L}{c}(n_g - 1) \quad (10)$$

The rotary photo drag is written as:

$$\theta_d = \frac{L\omega_s}{c} \left( n_g - \frac{1}{n_r} \right) \quad (11)$$

The cross-sectional area of a particle is written as:

$$\sigma_{scr} = \frac{2\pi^5 d^6}{3\lambda^4} \left( \frac{n_r - 1}{n_r + 2} \right)^2 \quad (12)$$

Here,  $d$  is the diameter of a spherical particle, while  $\lambda$  is wavelength of light denoted by  $\lambda = 2\pi c/\omega$ .

The scattering cross-sectional sensitivity is written as:

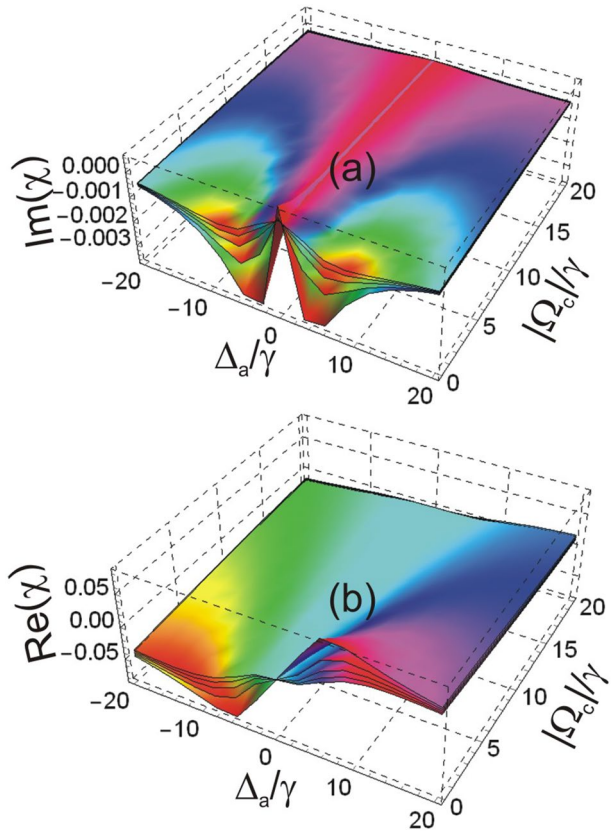
$$S_\sigma = \frac{\partial}{\partial n_r} \sigma_{scr} \quad (13)$$

### 3 Results and discussions

To address the issues of IoT devices and communication that were discussed in the previous sections, this portion provides an explanation of the graphical results for subluminal/superluminal propagation, rotating photon drag, scattering cross-section, and its sensitivity in the atomic medium. It is decided that the decay rate, denoted by “ $\gamma$ ,” will be  $2\pi$  GHz, and then other frequency-dependent parameters will be evaluated in relation to this decay rate. Other parameters are; the light speed in free space  $c = 3 \times 10^8$  m/s, the plank constant in reduced form  $\hbar = 1.05 \times 10^{-34}$  Js, the free space permittivity  $\epsilon_0 = 8.85 \times 10^{-12}$  F/m and atomic density  $N = 10^{23}$  atom/cm<sup>3</sup>. The formula for determining the wavelength is as follows:  $\lambda = 2\pi c/\omega$ , with the assumption that the angular frequency is  $\omega = 1000\gamma$ . In this manuscript, we show that the absorption, dispersion, group index, delay time, photon drag, scattering cross-section, and scattering cross-sectional sensitivity are interrelated to each other. For large values of absorption, amplification, and gain, these parameters are large and for small values of absorption, amplification, and gain, these parameters have small values.

Plots for the electric susceptibility of the medium versus the detuning of the cavity mode from an atomic transition denoted by  $\Delta_a/\gamma$  and the Rabi frequency of the control

**Fig. 3** Absorption and dispersion versus  $\Delta_a/\gamma$  and  $|\Omega_c|/\gamma$  such as  $\Delta_c = 0\gamma$ ,  $\delta = 0\gamma$ ,  $\varphi = 0$ ,  $G = 1.3\gamma$ ,  $n = 5, 10, 15, 20, 25$

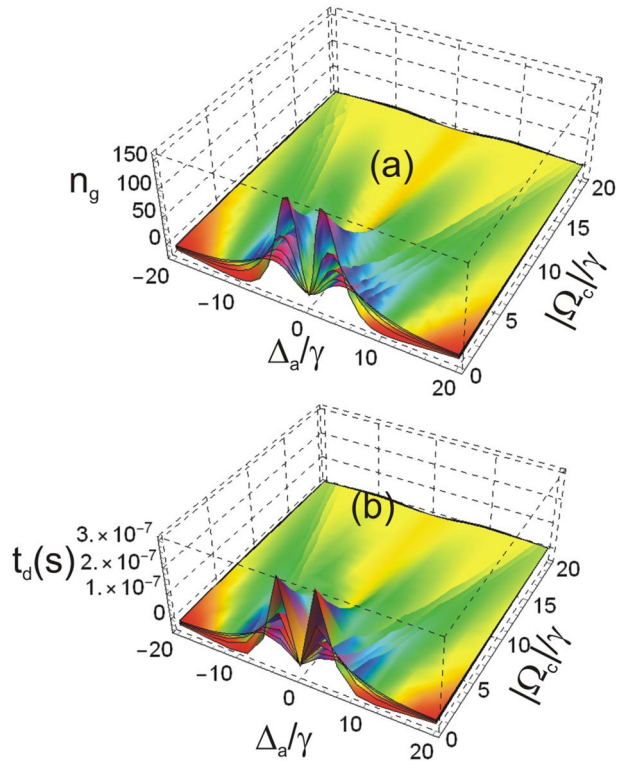


field denoted by  $|\Omega_c|/\gamma$  are presented in Fig. 3. While the real part of the electric susceptibility, denoted by  $Re(\chi)$ , is associated with the absorption spectrum in the atomic medium. The absorption is very close to zero when  $\Delta_a = 0\gamma$ , but it shifts to a negative value as the control field Rabi frequency  $|\Omega_c|/\gamma$  is increased in value. The absorption has a negative value of  $-0.00035\text{aru}$  at the place where  $\Delta_a = \pm 5\gamma$  is located. The phenomenon known as amplification results from negative absorption and may have some use in the development of superconducting devices.

We can control the absorption of the probe field through the detuning, control field Rabi frequency, and photon number density. The low absorption minimizes the losses in the medium and enhances the system’s efficiency. The negative absorption or amplification is reduced with  $n = 5$  to  $n = 10, 15, 20$  and then to  $n = 25$  as given by Fig. 3a. The dispersion spectrum is flat at  $\Delta_a = 0\gamma$  and the group index is equal to the refractive index at that point  $\Delta_a = 0\gamma$ . The dispersion is normal at the points  $\Delta_a = \pm 5\gamma$  and decreases its anomalous behavior with the Rabi frequency of the control field, as well as photon number density  $n = s, 10, 15, 20, 25$  as shown in Fig. 3b. The graphs that represent the group index and the delay time of the medium are plotted against the detuning of the cavity mode resulting from the atomic transition  $\Delta_a/\gamma$  and the Rabi frequency of the control field  $|\Omega_c|/\gamma$  in Fig. 4. The group index is also connected to the group velocity “ $v_g$ ”, which is measured

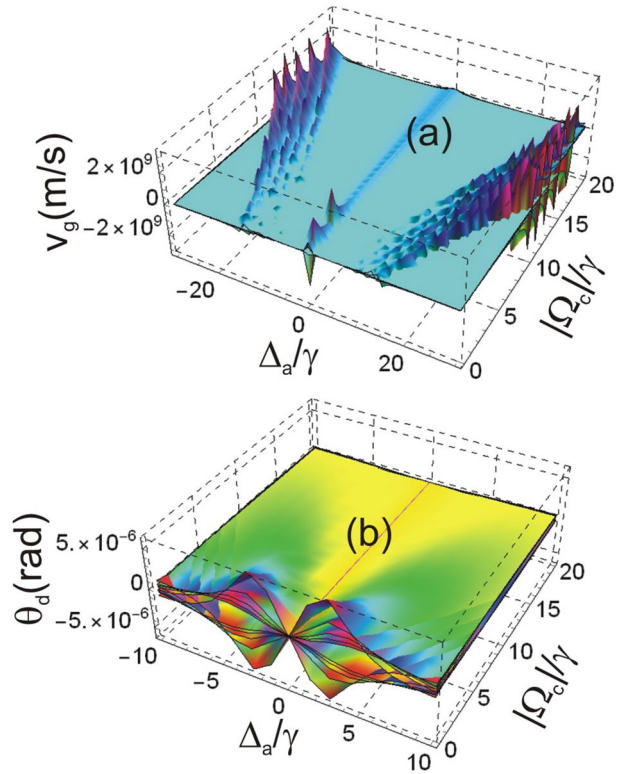


**Fig. 4** Group index and the delay time, versus  $\Delta_a/\gamma$  and  $|\Omega_c|/\gamma$  such as  $\Delta_c = 0\gamma$ ,  $\delta = 0\gamma$ ,  $\varphi = 0$ ,  $G = 1.3\gamma$ ,  $n = 5, 10, 15, 20, 25$



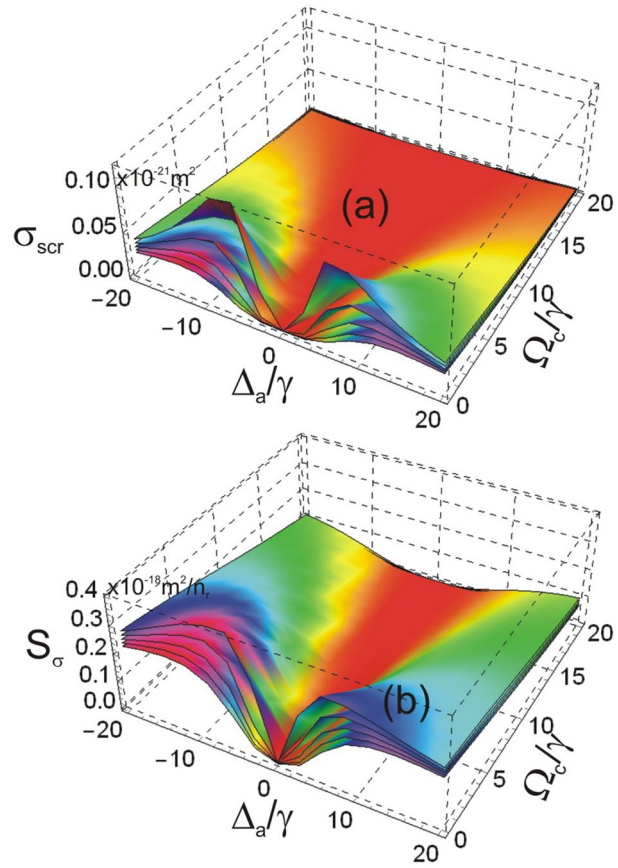
in the medium  $v_g = c/n_g$ . When the group index is positive, the velocity of the group will be low, indicating subluminal propagation. In this case, the value of the group index is almost identical to the value of the refractive index, as indicated by the equation  $n_g = n_r$  when  $\Delta_a = 0\gamma$  is satisfied. As a result of their being zero dispersion, the group velocity of the pulse is the same as the phase velocity in this scenario. At the parameter setting of  $\Delta_a = \pm 5\gamma$ , the group index is improved to a positive value of  $n_g = 150$ . When  $\Delta_a = \pm 20\gamma$  and  $10\gamma \leq |\Omega_c| \leq 20\gamma$  are reached, the value of the group index falls below the value of the unit value. In Fig. 4a, the group index will drop as the photon number density increases from  $n = 5, 10, 15, 20, 25$ , respectively. A quantum effect known as delay time is implemented in chips and other small IoT devices in order to boost their capacity for data storage. In addition, the amount of delay time plays a role in determining the pace at which data is transferred between IoT devices. The delay time is calculated by subtracting the amount of time required for a pulse to travel through a medium from the amount of time required for the same pulse to travel through free space for the same length  $L$ . At the region of significant amplification, which occurs at  $\Delta_a = \pm 5\gamma$  and low control field Rabi frequency  $|\Omega_c| < 5\gamma$ , the delay time is positive. The maximum amount of delay time happens when  $\Delta_a = \pm 5\gamma$  and the low control field Rabi frequency  $|\Omega_c| = 3.5\gamma$ , the value of which is equivalent to  $t_g = 0.3\mu s$ . The minimal amount of delay time happens when  $\Delta_a = 0\gamma$ , and the low control field Rabi frequency  $|\Omega_c| < 5\gamma$ , whose value gets closer and closer to  $t_g \sim 0$ . As can be seen in Fig. 4b, the delay time gets shorter as the photon number density gets higher  $n = 5, 10, 15, 20, 25$  and as the control field Rabi frequency gets higher  $|\Omega_c|/\gamma$ .

**Fig. 5** Group velocity and rotary photon Drag versus  $\Delta_a/\gamma$  and  $|\Omega_c|/\gamma$  such as  $\Delta_c = 0\gamma$ ,  $\delta = 0\gamma$ ,  $\varphi = 0$ ,  $G = 1.3\gamma$ ,  $n = 5, 10, 15, 20, 25$



In Fig. 5, the plots are depicted for the group velocity and rotary photon drag versus detuning of the cavity mode from atomic transition  $\Delta_a/\gamma$  and the Rabi frequency of the control field  $|\Omega_c|/\gamma$ . The group velocity is the speed at which data transfer takes place in an IoT device. The group velocity is nearly equal to the vacuum velocity of light  $v_g = c$  at  $\Delta_a = 0\gamma$ . The group reduced to the value of  $c/n_g = 2 \times 10^6 m/s$  at  $\Delta_a = \pm 5\gamma$ . The value of group velocity enhanced to the value of  $c/n_g = \pm 2 \times 10^9 m/s$  at  $\Delta_a = \pm 20\gamma$  and  $10\gamma \leq |\Omega_c| \leq 20\gamma$ . This is a superluminal effect that indicates highly efficient data transmission and signal processing. Further, the group velocity increases with the photon number density of  $n = 5, 10, 15, 20, 25$  as by Fig. 5a. When a light beam enters to a rotatory medium along its axis, it is dragged in the same or opposite direction of the spinning velocity of the medium. This phenomenon is called photon drag. Here, the photon is dragged in the same direction as that of the spinning velocity, in the region of  $\Delta_a = \pm 5\gamma$ . When the spinning velocity is positive such as  $\omega_s = 20 rad/s$  (mean clockwise), the drag is positive such as  $\theta_d = 5$  microradian (clockwise). But when the spinning velocity is negative such as  $\omega_s = -20 rad/s$  (anticlockwise), the drag is positive such as  $\theta_d = -5$  microradian (anticlockwise). This means that, for slow light, the pulse is dragged in the same direction as the spinning velocity of the medium. In the region of  $\Delta_a = \pm 20\gamma$  and  $10\gamma \leq |\Omega_c| \leq 20\gamma$ , the group velocity is more than the vacuum speed of light. In this case, the spinning velocity is positive such as  $\omega_s = 20 rad/s$  (mean clockwise), the drag is negative (anticlockwise) and the spinning velocity is negative such as  $\omega_s = -20 rad/s$

**Fig. 6** Scattering cross-section area and sensitivity cross section area with respect to refractive index versus  $\Delta_a/\gamma$  and  $|\Omega_c|/\gamma$  such as  $\Delta_c = 0\gamma$ ,  $\delta = 0\gamma$ ,  $\varphi = 0$ ,  $G = 1.3\gamma$ ,  $n = 5, 10, 15, 20, 25$



(anticlockwise), the drag is negative (clockwise). Further, the photon drag is reduced with increasing photon number density in a cavity as shown in Fig. 5b.

In Fig. 6, the plots are given for scattering cross-section of small particles. The scattering cross-section of small particles is a function of detuning of the cavity mode from atomic transition  $\Delta_a/\gamma$  and the Rabi frequency of the control field  $|\Omega_c|/\gamma$ . The scattering is negligible at  $\Delta_a = 0\gamma$  and low value of  $|\Omega_c| < 5\gamma$ . The cross-section has a high value of at  $\Delta_a = \pm 10\gamma$  and low control field Rabi frequency  $|\Omega_c| < 5\gamma$ . The value of cross-section at this point is  $\Delta_a = 0\gamma$  and low control field Rabi frequency  $0.1 \times 10^{-21} m^2$ . The cross-section decreases with both the increase of photon number density as well as the Rabi frequency of the control field, as illustrated in Fig. 6a. In quantum-based IoT, there are instances where electromagnetic waves interact with objects or structures, resulting in various phenomena such as signal attenuation, reflection, or interference. These interactions impact the efficiency and reliability of wireless communication systems and quantum-based IoT devices. The cross-section per unit refractive index in the medium is called cross-sectional interrogation of sensitivity. The cross-sectional interrogation of sensitivity is also a function of detuning the cavity mode from atomic transition  $\Delta_a/\gamma$  and control field Rabi frequency  $|\Omega_c|/\gamma$ . The cross-sectional interrogation of sensitivity is minimum at  $\Delta_a = 0\gamma$  at low control field having Rabi frequency

of  $|\Omega_c| < 5\gamma$ . The cross-sectional interrogation of sensitivity is the maximum value of  $S_\sigma = 0.4 \times 10^{-19} m^2/n_r$  at  $\Delta_a = \pm 10\gamma$  and  $|\Omega_c| = 3.5/\gamma$ . The cross-sectional interrogation of sensitivity decreases with both the photon number density  $n = 5, 10, 15, 20, 25$  and the control field having a Rabi frequency of  $|\Omega_c|/\gamma$  as given by Fig. 6b. In the case of quantum-based IoT, the atoms are considered as the building blocks for sensors that can measure physical quantities like temperature, magnetic fields, electric fields, and pressure at the quantum level, by precisely manipulating and controlling the quantum states of these atoms.

### 4 Deployment and work of proposed model in sensors and IoT

Here, we detail how the suggested quantum-based approach can be implemented in IoT sensors. The following three subsections explain the employment of our scheme.

#### 4.1 Applications and use of photon drag in IoT

We investigated the rotary photon drag to  $\theta_d = \pm 5$  micro radian. This effect of photon drag is used in sensing, energy harvesting, and optical switching in IoT. In optical switching, an external field (mostly a laser beam) exerts a force on the atoms, which is used for the manipulation of the position as well as the movement of these atoms. On the basis of this property, optical switches (re-configurable optics) are made for the IoT devices used for the control and modulation of signals dynamically. The use of photon drag in optical switching, and its work process in IoT is illustrated in Fig. 7.

In wired/wireless communication for IoT, optical switching provides higher bandwidth, compared to traditional ones. This enables the transfer of bulk data among IoT devices. It also makes possible HD-streaming as well as can handle data from multiple sources, at the same time. Further, the delay time is also minimized and the communication in IoT is made real-time.

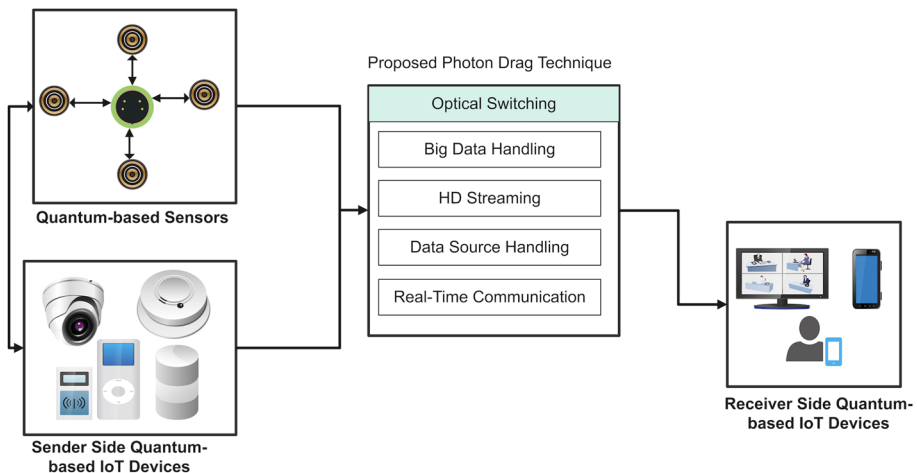


Fig. 7 Optical switching and its work process in IoT

## 4.2 Applications of scattering cross section in IoT

The scattering cross-section of  $0.1 \times 10^2 \text{ m}^2$  is measured. In quantum, the scattering cross-section refers to the phenomenon describing the interaction between electromagnetic waves and particles/atoms. As a result of this interaction, many phenomena occur such as interference of signals, reflection, or signal attenuation. Hence, this phenomenon greatly affects the efficiency as well as the reliability of communication in IoT, based on quantum. To counter the problem of signal interference, this effect is used as shown in Fig. 8. It reduces the blockage of signals and increases its propagation. Using the diversity technique of scattering cross-section, the effect of multi-path fading is reduced to avoid conjunction.

## 4.3 Applications of scattering cross sectional sensitivity in IoT and sensors

We measured the maximum cross-sectional sensitivity of  $S_\sigma = 0.4 \times 10^{-19} \text{ m}^2/n_r$ . For the communication in IoT to be secure, the cross-sectional sensitivity of atoms plays a major role as it enables the sensors to detect with high precision. In quantum-based IoT, it is the ability of atoms/quantum systems to precisely detect external influences and respond to them. The atoms are considered as the basis for quantum sensors for the measurement of temperature, pressure, magnetic as well as electric field at the quantum level which manipulate the atom's quantum states. Further, quantum-based cryptography, like quantum key distribution (QKD) enables secure communication channels, having high resistance to eavesdroppers, as provided by Fig. 9.

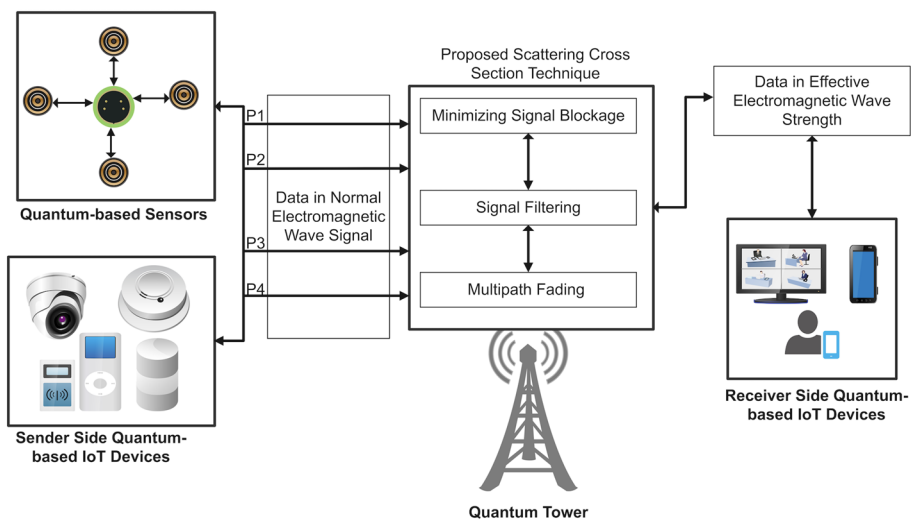


Fig. 8 Scattering cross section in IoT

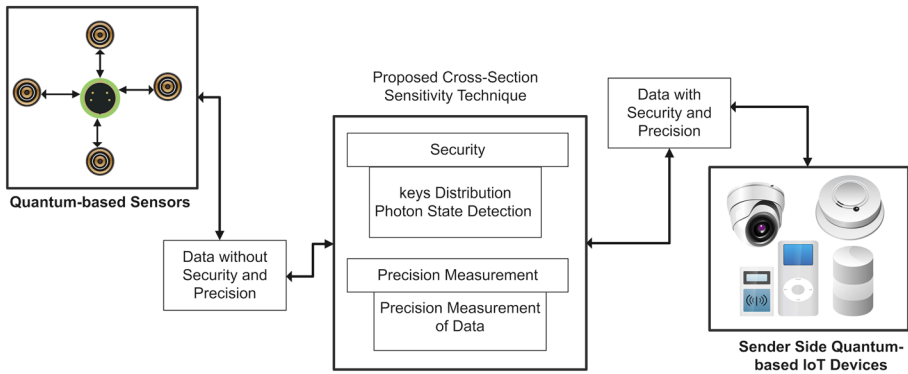


Fig. 9 Scattering cross-sectional sensitivity in IoT and Sensors

## 5 Conclusion

In this paper, a two-level atom-cavity coupling system is employed for the purpose of modifying optical responses as well as the scattering cross-section and related scattering sensitivity. In a two-level atomic medium connected with a cavity, it is possible to regulate and modify the subluminal/superluminal propagation of light, as well as rotating photon drag, scattering cross-section, and the system's sensitivity. For the purpose of deriving optical susceptibility and the related formulas of refractive and group index, group velocity, photon drag, and scattering cross-section of the particle, as well as scattering cross-sectional sensitivity with regard to refractive index, the density matrix formalism is utilized. In the region of substantial amplification, it has been reported that the sensitivity of the group index, delay time, photon drag, and scattering cross-sectional area is large, and the contrast behavior has been seen in this region. The range of values that are reported for the group index is between  $-0.1 \leq n_g \leq 150$ , and the range of values that are reported for the group velocity is between  $2 \times 10^6 \text{ m/s} \leq v_g \leq \pm 2 \times 10^9 \text{ m/s}$ . It has been stated that the greatest delay time is  $t_g = 0.3 \mu\text{s}$ , and the rotary photon drag is claimed to be  $\theta_{\text{rot}} = \text{pm}5$  micro radian. The Internet of Things takes advantage of a phenomenon known as photon drag for sensing, energy harvesting, and optical switching. It has been determined that the scattering cross-section is  $0.1 \times 10^{21} \text{ m}^2$ . The scattering cross-section can affect the effectiveness and reliability of quantum-based communication for the IoT. The greatest sensitivity of the cross-section was measured to be  $S_\sigma = 0.4 \times 10^{-19} \text{ m}^2/n_r$ . The cross-sectional sensitivity may affect the secure transmission and extremely accurate detection capabilities of sensors and the IoT. Within the atom-cavity coupling concept framework, the subluminal propagation, rotational photon drag, and cross-sectional sensitivity of particles all decrease with an increase in the number of photons.

**Acknowledgements** The researchers would like to acknowledge the Deanship of Scientific Research, Taif University for funding this work.

**Author Contributions** SSU and AK, conceived and designed the model, analyzed the data, and wrote the manuscript. SH assisted with model design, conducted statistical analyses, and contributed to manuscript revisions. MA, RA, and SA provided guidance and expertise in the study design and critically reviewed the manuscript for important intellectual content. All authors have read and approved the final version of the manuscript.

**Funding** Open access funding provided by University of Agder.

**Data availability** The data generated and/or analyzed during the current study are available from the corresponding author upon reasonable request.

## Declarations

**Conflict of interest** The authors declare that they have no competing interests that could have influenced the design, implementation, analysis, or reporting of this study. There are no financial, personal, or professional relationships that could be perceived as potential conflicts of interest.

**Ethical approval** Ethical approval was not required for this study as it did not involve the use of human or animal subjects.

**Open Access** This article is licensed under a Creative Commons Attribution 4.0 International License, which permits use, sharing, adaptation, distribution and reproduction in any medium or format, as long as you give appropriate credit to the original author(s) and the source, provide a link to the Creative Commons licence, and indicate if changes were made. The images or other third party material in this article are included in the article's Creative Commons licence, unless indicated otherwise in a credit line to the material. If material is not included in the article's Creative Commons licence and your intended use is not permitted by statutory regulation or exceeds the permitted use, you will need to obtain permission directly from the copyright holder. To view a copy of this licence, visit <http://creativecommons.org/licenses/by/4.0/>.

## References

- Ageed, Z.S., Zeebaree, S.R.M., Saeed, R.H.: Influence of quantum computing on IoT using modern algorithms. In: 2022 4th international conference on advanced science and engineering (ICOASE), Zakho, Iraq, pp. 194–199, (2022)
- Arif, S.M., Bacha, B.A., Wahid, U., Haneef, M., Ullah, A.: Tunable subluminal to superluminal propagation via spatio-temporal solitons by application of laguerre fields intensities. *Phy. Lett. A* **388**, 127041 (2021)
- Arif, S.M., Bacha, B.A., Wahid, U., Ullah, A., Haneef, M.: Tunnelling based birefringent phase sensitivity through dynamic chiral medium. *Phys. Scr.* **96**, 035106 (2021)
- Butt, M.A., Kazanskiy, N.L., Khonina, S.N., Voronkov, G.S., Grakhova, E.P., Kutluyarov, R.V.: A review on photonic sensing technologies: status and outlook. *Biosensors* **13**, 568 (2023)
- Chawla, D., Mehra, P.S.: A survey on quantum computing for internet of things security. *Procedia Comput. Sci.* **218**, 2191–2200 (2023)
- Costa, F., Traoré-Dubuis, A., Álvarez, L., Lozano, A.I., Ren, X., Dorn, A., Limão-Vieira, P., Blanco, F., Oller, J.C., Muñoz, A., et al.: A complete cross section data set for electron scattering by pyridine: modelling electron transport in the energy range 0–100 eV. *Int. J. Mol. Sci.* **21**, 6947 (2020)
- Karim, F., Haneef, M., Ullah, S.S., et al.: Manipulation speed of light and giant phase shifting: a new quantum-based model for improving efficiency and security of internet of things. *Opt. Quant. Electron.* **55**, 796 (2023)
- Li, Z., et al.: Entanglement-assisted quantum networks: mechanics, enabling technologies, challenges, and research directions. In: *IEEE communications surveys tutorials* (2023)
- Saushin, A.S., Mikhchev, G.M., Vanyukov, V.V., Svirko, Y.P.: The surface photogalvanic and photon drag effects in Ag/Pd metal-semiconductor nanocomposite. *Nanomaterials* **11**(11), 2827 (2021)
- Xu, G., Mao, J., Sakk, E., Wang, S.P.: An overview of quantum-safe approaches: quantum key distribution and post-quantum cryptography. In: 2023 57th annual conference on information sciences and systems (CISS), Baltimore, MD, USA, pp. 1–6, (2023)

**Publisher's Note** Springer Nature remains neutral with regard to jurisdictional claims in published maps and institutional affiliations.

## Authors and Affiliations

Syed Sajid Ullah<sup>1</sup> · Aizaz Khan<sup>2</sup> · Saddam Hussain<sup>3</sup> · Majed Alsafyani<sup>4</sup> ·  
Roobaea Alroobaea<sup>4</sup> · Sultan Algarni<sup>5</sup>

✉ Syed Sajid Ullah  
syed.s.ullah@uia.no

Aizaz Khan  
aizazoptics@gmail.com

Saddam Hussain  
saddamicup1993@gmail.com

Majed Alsafyani  
alsufyani@tu.edu.sa

Roobaea Alroobaea  
r.robai@tu.edu.sa

Sultan Algarni  
saalgarni@kau.edu.sa

<sup>1</sup> Department of Information and Communication Technology, University of Agder,  
N-4898 Grimstad, Norway

<sup>2</sup> Department of Physics, University of Malakand, Chakdara, Khyber Pakhtunkhwa, Pakistan

<sup>3</sup> School of Digital Science, Universiti Brunei Darussalam, Jalan Tungku Link, Gadong BE1410,  
Brunei

<sup>4</sup> Department of Computer Science, College of Computers and Information Technology, Taif  
University, P.O. Box 11099, 21944 Taif, Saudi Arabia

<sup>5</sup> Department of Information Systems, Faculty of Computing and Information Technology, King  
Abdulaziz University (KAU), 21589 Jeddah, Saudi Arabia